INTERNATIONAL JOURNAL OF OPTIMIZATION IN CIVIL ENGINEERING
Int. J. Optim. Civil Eng., 2021; 11(4): 647-661

OPTIMAL SINGLE AND MULTIPLE TUNED MASS DAMPERS BASED ON NONLINEAR STRUCTURES RESPONSES USING THE MOUTH BROODING FISH ALGORITHM

E. Jahani[1] and M. Roozbahan[2*, †]
[1]*Department of Civil Engineering, University of Mazandaran, Babolsar, Mazandaran, Iran*
[2]*Department of Civil Engineering, Izmir Institute of Technology IYTE, Urla, Turkey*

ABSTRACT

The multiple tuned mass dampers (MTMDs) are considered among the control systems used for reducing the vibration of buildings under seismic excitations. A large number of the previous studies have mainly emphasized on the utilization and effectiveness of MTMD on linear structure responses, and few of them have investigated the effectiveness of MTMD on nonlinear multi-degree of freedom structures. Thus, in this paper, the effectiveness of MTMD on nonlinear buildings have been investigated. The effectiveness of the MTMD systems lies in their parameters, and the location of dampers in buildings. Accordingly, the optimization of MTMD's properties, as well as its location, are taken into account in the present study. The Mouth Brooding Fish algorithm, which is a new optimization method is utilized for optimizing the properties corresponding to the MTMD system. The effectiveness levels of the MTMDs were compared with the efficiency of an equal optimally tuned mass damper (TMD), which was placed on the top of the building. The results of these comparisons revealed that MTMDs have provided a better efficiency compared to TMDs in reducing the maximum displacement of nonlinear structures. Moreover, MTMDs have a higher effectiveness when placed on different floors of the building.

Keywords: multiple tuned mass damper; nonlinear; structural control; optimization; mouth brooding fish algorithm.

Received: 12 July 2021; Accepted: 14 November 2021

1. INTRODUCTION

To protect structures against wind and earthquake loadings, different structural control

[*]Corresponding author: Department of Civil Engineering, Izmir Institute of Technology IYTE, Urla, Turkey
[†]E-mail address: mroozbahan@iyte.edu.tr (M. Roozbahan)

mechanisms have been proposed. The tuned mass damper (TMD) devices are known as the systems most widely used to protect towers against vibrations due to their effectiveness in seismic and wind load vibration control [1,2]. Some of the examples include Air Traffic Control Tower in Delhi 2015, Taipei 101 in Taiwan 2004, Spire of Dublin in Dublin 2003, One Wall Centre Tower in Vancouver 2001, Millennium Bridge in London 2001, and Burj Al-Arab in Dubai 1999 [3]. A TMD consists of mass, damper, and stiffness members [4].

The primary form of the tuned mass damper was invented by Frahm in 1909 for reducing the resonance vibrations by using an additional mass [5]. Ormondroyd and Den Hartog attached damping elements to Frahm's device to damp vibrations since it was not applicable when subjected to excitation with variable frequencies [6]. Sacks et al. demonstrated the TMD performance in reducing the displacement of towers and buildings [7]. Elias and Matsagar investigated the TMD's effect on the responses of tall buildings, where the TMD was installed on different floors of the building [8]. Abd-Elhamed and Mahmoud have performed a study on the TMD efficiency in reducing the building's dynamic response to the far-field earthquake and near-field earthquake records such as the effects of soil-structure interaction [9]. Gwalani and Jaiswal studied the effect of an elastoplastic tuned mass damper on an elastic and an elastoplastic single degree of freedom structures (SDOFs) under harmonic base excitations and seismic ground motions [10].

In tall buildings, the installation of a single TMD may take remarkable space and a heavy mass for installation. Also, a single TMD tuned to the higher mode's vibration play a critical role in the total response of high-rise building, while the first mode of vibration may not have a considerable impact on total response [11]. To overcome these defects, Xu and Igusa proposed multiple tuned mass dampers (MTMDs). Based on the results of this study, optimally designed MTMD can prove to be more robust and efficient than an optimally designed TMD with an identical total mass [12]. According to Li, optimum MTMDs have outperformed the optimal TMD and have demonstrated more robustness than TMD [13]. Zuo showed the performance of various MTMDs in structural response control. According to his report, MTMDs outperform different types of TMDs with a similar mass ratio [14]. Steinbuch has conducted a study applying the bionic optimization method for amplifying the TMD performance in mitigating the response of the structures exposed to earthquake motions. It was proved that MTMDs were more efficient than TMD in structural response control with optimal damper parameters [15].

Mohebbi et al. indicated the optimum MTMD's efficiency in *structural response control* of buildings exposed to earthquake ground motions. Based on their findings, an increase in the mass ratio will contribute to an improvement in MTMD performance [16]. Frans and Arfiadi studied the optimized properties and location of MTMD in three and ten-story buildings using the genetic algorithm [17]. Based on a report by Sakr, an increase in the number of floors employed as TMDs and story mass ratios will contribute to a more considerable enhancement in the wind- and the earthquake-excited response of structures [18]. Rahman et al. compared the effectiveness of TMD and MTMD on a 10-story building. According to their reports, MTMD that had been located in different stories had more efficient [19]. Suresh and Mini investigated the effectiveness of single and multiple tuned mass dampers on three and five degrees of freedom frames. According to the results, increasing the number of TMDs offers reductions in the maximum displacement of structures [20].

The majority of studies have solely focused on the effect of multiple tuned mass dampers on linear structures, and none of them has evaluated the effectiveness of MTMDs on nonlinear multi-degree of freedom structures (MDOFs). In the present study, the effects of optimal MTMDs on nonlinear MDOFs have been analyzed and compared with the effects of optimal TMDs on nonlinear MDOFs. To optimize the parameters of single and multiple tuned mass dampers, including mass and stiffness, the Mouth Brooding Fish (MBF) algorithm was used. This algorithm has provided a better performance compared to other optimization methods.

This paper is *structured* in the following way: Section 2 introduces the equation of motion of a nonlinear multi-degree of freedom structure equipped with MTMD and subjected to earthquake excitation. An overview of the Mouth Brooding Fish algorithm is presented in Section 3. Section 4 develops the MBF algorithm for the optimal design of single and multiple tuned mass dampers in nonlinear multi-degree of freedom structures exposed to seismic excitations. Sections 5 verifies the program of nonlinear analysis and MTMDs optimization. Section 6 compares the effectiveness of optimal single and multiple tuned mass dampers optimized using the Mouth Brooding Fish algorithm for reducing the responses of nonlinear structures. Finally, Section 7 represents the conclusions.

2. STRUCTURE-MTMD EQUATION OF MOTION

The equation of motion for an n-degree of freedom structure equipped with TMDs, which is subjected to earthquake, $\ddot{x_g}$, is given by:

$$[M]\ddot{x}(t) + [C]\dot{x}(t) + [K]x(t) = -[M]e\ddot{x}_g(t) \tag{1}$$

where [M], [C], and [K] are the mass, damping, and stiffness matrices of the system, respectively. X indicates displacement, $\dot{x}$ indicates velocity, and $\ddot{x}$ indicates acceleration vectors relative to ground motion. $e^T = [-1, \ -1, \ \cdots, \ -1]_{1\times(n+N_{tmd})}$ is the ground acceleration mass transformation vector. A model of multiple degrees of freedom structure equipped with MTMD is shown in Fig. 1.

The system in [M] matrix is given by Fig. 1:

$$[M] = [M_1, \ \cdots, \ M_N, \ m_{11}, \ \cdots, \ m_{1K}, \ m_{21}, \ \cdots, \ m_{2K}, \ \cdots, \ m_{N1}, \ \cdots, \ m_{NK}] \tag{2}$$

where M is the mass of each floor of the structure and m is the mass of each damper. The symbol m_{NK} indicates the mass for the damper in the K^{th} group located on the N^{th} floor.

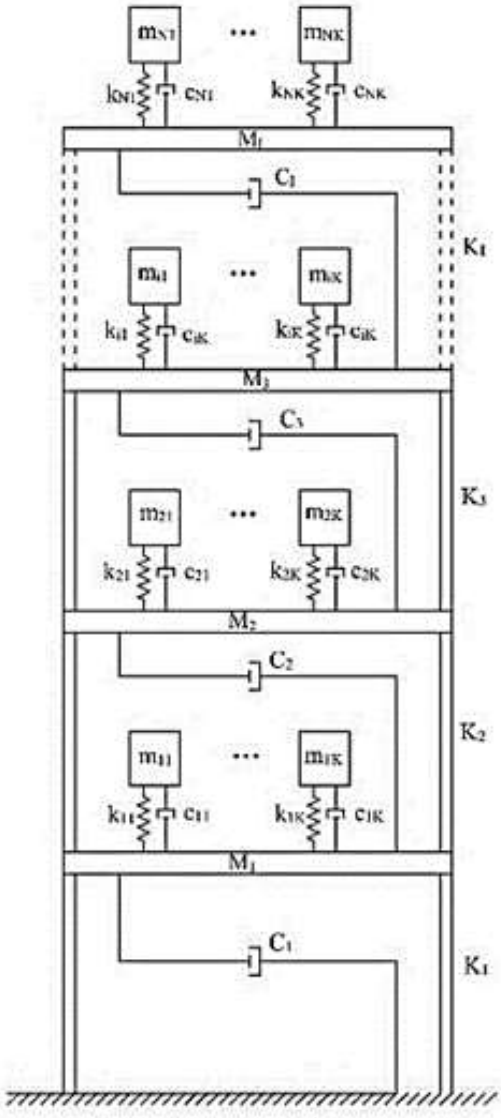

Figure 1. The model of the structure with MTMD

The stiffness matrix of the study system is given by:

$$K = \begin{bmatrix} K + k1 & k^{*} \\ k^{*T} & k \end{bmatrix} \tag{3}$$

where K is the stiffness matrix of the structure.

$$K=\begin{bmatrix} K_1+K_2 & -K_2 & 0 & 0 \\ -K_2 & K_2+K_3 & -K_3 & 0 \\ 0 & -K_3 & \cdots & -K_N \\ 0 & 0 & -K_N & K_N \end{bmatrix} \tag{4}$$

And the matrices k_1 and k^* are expressed as follows:

$$k1=diag\left[k_{11}+k_{12}+\ldots+k_{1K},\quad k_{21}+k_{22}+\ldots+k_{2K},\quad \ldots,\quad k_{N1}+k_{N2}+\ldots+k_{NK}\right] \tag{5}$$

$$k^*=\begin{bmatrix} -k_{11} & -k_{12} & \ldots & -k_{1K} & & & & & & & & \\ & & & & -k_{21} & -k_{22} & \ldots & -k_{2K} & & & & \\ & & & & & & & & \ddots & & & \\ & & & & & & & & & -k_{N1} & -k_{N2} & \ldots & -k_{NK} \end{bmatrix} \tag{6}$$

As mentioned above, the symbol k_{NK} is the stiffness of a damper in the K^{th} group placed on the N^{th} floor.

Also, k is the diagonal matrix and is in the following form:

$$k=\left[k_{11},\quad k_{12},\quad \ldots,\quad k_{1K},\quad k_{21},\quad k_{22},\quad \ldots,\quad k_{2N},\quad \ldots,\quad k_{N1},\quad K_{N2},\quad \ldots,\quad k_{NK}\right] \tag{7}$$

It is worth mentioning that the form of the damping matrix for System C is relatively similar to the form of the stiffness matrix K [21].

The stiffness of degrees of freedom is not constant in an elastoplastic system; this value is influenced by the importance of the system's resisting force in each phase considering the chronicles of movements. In the nonlinear stiffness model of bilinear elastoplasticity shown in Fig. 2, f_s, f_y, and u_y represent resisting force, yield force, and yield distortion, respectively.

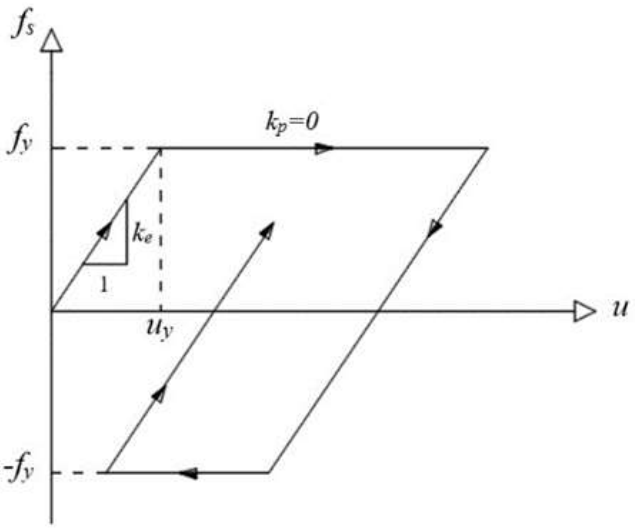

Figure 2. Nonlinear bilinear elastoplastic stiffness model

The amount of stiffness in every time lag is directly correlated with the ratio of resisting force of the system's degrees of freedom to its yield force (f_s/f_y). If this ratio is less than one, degrees of freedom behave is elastic and k_e must be considered as the stiffness value in computations if it is equal to one, we are facing with an elastoplastic condition that k_p will be given as the stiffness value. Newmark's constant average acceleration approach can be utilized to compute the movement equation [22].

3. MOUTH BROODING FISH ALGORITHMS

The mouth brooding fishes' movements in the survival pattern of their children's and their life course is the foundation for the MBF algorithm. For having the best answer by the MBF algorithm in this problem, all impacts on movements of cichlids should be taken into account. Some of these movements are the effects of a shark attack on movements of cichlids, Roulette Wheel selection, the additional movements of left-out cichlids, and the basic movements of each cichlid. Each cichlid has some fundamental movements [23].

Their main factors are defined as follows: The effect of the strength of the mother on cichlid movements is the first factor. The next one is the optimized position for cichlids. Each cichlid wants to reach an optimized position. They go through iterations that are far from their current position and reach the optimized position. The disposition of all children in order for reaching the optimized position for all cichlids is another factor for the movement. And finally, the trends or natural forces are the last factors in the fundamental movements. Natural trends or forces are obtained from past generations to current generations in the MBF algorithm. In the fundamental cichlids' movements, each cichlid can move up to another surrounding dispersion positive (ASDN) or additional surrounding dispersion negative (ASDN) that is defined as:

$$ASDP = 0.1 \times (VarMax - VarMin), ASDN = -ASDP \tag{8}$$

where VarMin indicates the minimum boundary, and VarMax indicates the maximum boundary for the variation problem, respectively.

The second impact on the movements of cichlids is the additional movement from the left out cichlids. In nature, cichlids are kept and protected by their mothers. MBF algorithm shows the same manner. The capacity of the mother's mouth indicates the number of cichlids she can keep. The remaining cichlids are not protected by their mother, and they have to struggle with challenges by themselves. These cichlids are called left-out cichlids. These excluded cichlids have to survive in nature; therefore, they have to move beyond fundamental movements. The bounds for their movements are multiplied by four accordingly:

$$UASDP = 4 \times ASDP, UASD = -UASDP \tag{9}$$

where UASDP is the ultra-additional surrounding dispersion positive and UASDN is the ultra-additional surrounding dispersion negative bounds corresponding to the left out cichlids movement, which are shown in Fig. 3.

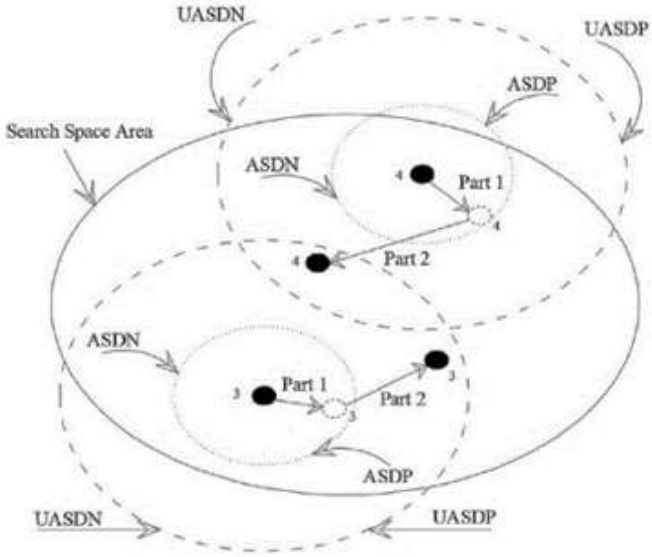

Figure 1. Left out cichlids' movements and limitations [23]

The third impact on the movement of cichlids is marriage. Some of the top cichlids are allowed to marry in MBF. Thus, utilizing some methods like Roulette Wheel selection or a probability distribution in MBF algorithm marriage can occur. The newly born cichlids will have new positions. They will occupy their parent's place in the population.

Another effect on the movement of cichlids is the impact of a shark attack. About 4 percent of every population or colony of cichlids is attacked by natural threats like sharks. Therefore, the shark attack effect is an additional movement for cichlids, which is used for that 4 percent in the MBF algorithm.

$$nshark = 0.04 \times nFish \tag{10}$$

where nFish indicates the size of the population of cichlids and nshark is the number of chosen cichlids for the shark attack effect.

4. MOUTH BROODING FISH ALGORITHMS FOR OPTIMIZATION OF MTMDS

To find the best possible model of TMDs and MTMDs, an optimization problem was developed considering minimizing the maximum structural displacement as the objective function as well as the constants of MTMDs (such as mass (m_d) and stiffness (k_d)) which were estimated as variables. Drawing the conventional optimization techniques was not advantageous since MTMD optimization requires certain parameters with broad variations; thus, a more efficient approach is needed. A variety of methods already have been launched to address nature-based optimization questions; Because of the merits in achieving global optimization and prompt convergence, global optimization algorithms such as the Genetic Algorithm [24-26], Particle Swarm Optimization [27-29], Charged System Search [30,31],

Cuckoo Search [32,33] and Harmony Search [34,35] have been given more credit, and their applications are common in civil engineering. For global optimization, the MBF algorithm has recently became recommended. In the present study, the MBF algorithm was applied to solve the optimization problem by analyzing the structural dynamic response. The flowchart of the program is given in Fig. 4.

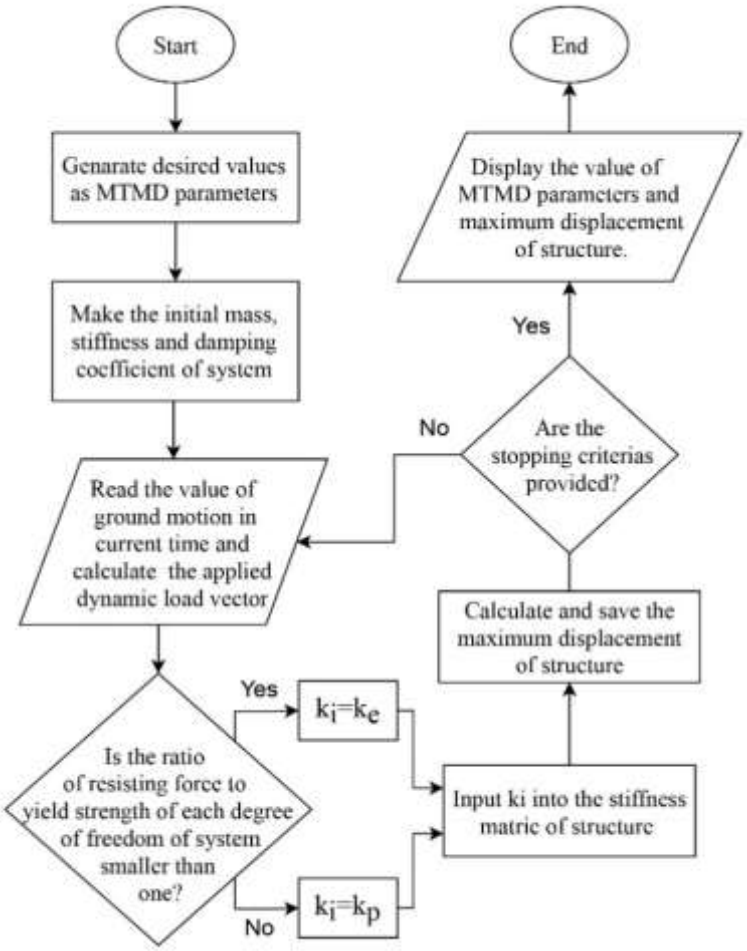

Figure 2. Flowchart of the program

5. VERIFICATION OF NUMERICAL ANALYSIS

5.1 Verification of TMD optimization

A comparison was done between the results of optimization of TMD using mouth brooding fish algorithm with the result of the other optimization methods including Genetic Algorithm (GA) [36], Charged System Search (CSS) [37], multi-objective cuckoo search (MOCS) [38], and Improved Harmony Search (IHS) [39] to verify this method. The results of the optimization of TMD on a ten-story structure which was taken from [40] are shown in

Table 1. The Imperial Valley Irrigation District (El Centro) 1940 NS ground acceleration record was used to analyze these examples. The maximum displacement of the uncontrolled structure under the El Centro earthquake is 0.1877 m.

Table 1: Verification of the presented method.

	GA [36]	CSS [37]	MOCS [38]	IHS [39]	MBF
Max Displacement (m)	0.1216	0.1224	0.1218	0.1208	0.1193
Percent of reduction	35.2	34.8	35.1	35.6	36.4
m_d (tons)	108	108	108	108	108
c_d (kN s/m)	151	88	160	122	57
k_d (kN/m)	3750	4207	4428	3654	3269

According to Table 1, The MBF algorithm had superior outcomes and was more efficient in diminishing the maximum structural displacement, compared to the other methods. Parameters of m_d=108 tons, c_d=57 kNs/m, and k_d=3269 kN/m were considered to be the optimal TMD values, which are significantly smaller than the amounts acquired by other approaches. The movement of the structure's top story, under the El Centro earthquake, either with or without TMD, can be seen in Fig. 5.

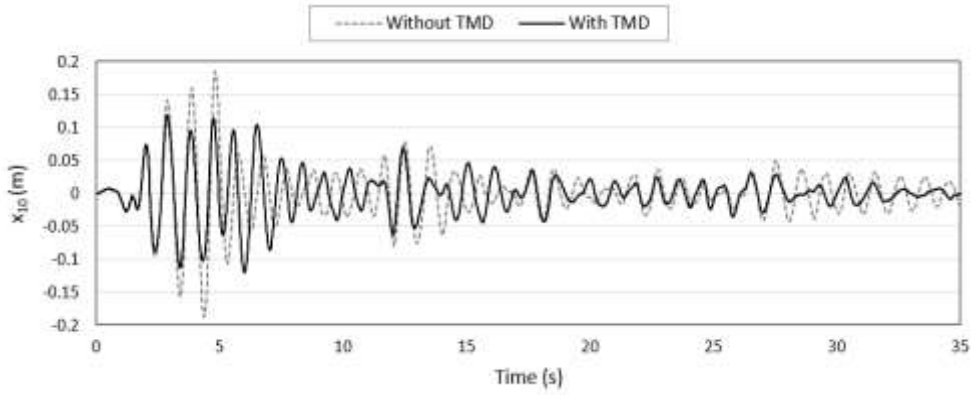

Figure 3. Displacement of the top story under the EI Centro NS earthquake record

5.2 Verification of nonlinear MDOF analysis

Referring to the example of nonlinear MDOF validation, a two-story building was used, which was previously studied by Jangid [41]. The elastic stiffness (k_e) of the first story is 394.784×10^3 N/m, and the first floor's mass is 5 tons, also the values of the second story's elastic stiffness and mass are half of the values of the first story. The building's columns have elastoplastic conduct with 0.05 m yield displacement. The responses of the second-floor displacement due to the 1940 earthquake ground movement of El-Centro, was evaluated. Fig. 6 demonstrate the outcomes of Jangid's evaluations and the developed program for analysis of nonlinear MDOF used in the paper.

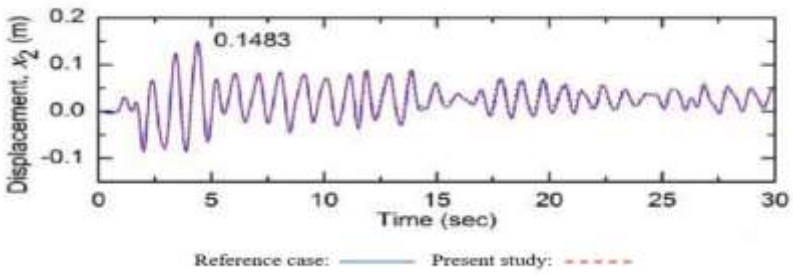

Figure 4. Time history of second story lateral displacement (nonlinear MDOF analysis verification)

The findings of the Jangid analysis and this paper are well-analogous, as shown in Fig. 6; this implies that the model functions perfectly in nonlinear analysis of structures by multi-degrees of freedom.

6. NUMERICAL STUDIES

In order to compare the effectiveness of single and multiple tuned mass dampers on nonlinear structure's response, a five-story building equipped with TMD and MTMD in three different situations has been studied. The distribution of dampers in the structures can be seen in Fig. 7. For each story of the structure, the elastic stiffness (k_e) was 3.404×10^5 kN/m, and plastic stiffness (k_p) was equal to 0, yielding occurred at the relative lateral displacement of $u_{yielding}$=0.024 m. Each floor mass was 354.6 tons. The linear viscous damping coefficient c was set 743.3 kNs/m for each story. The properties of each floor of the building were taken from [42].

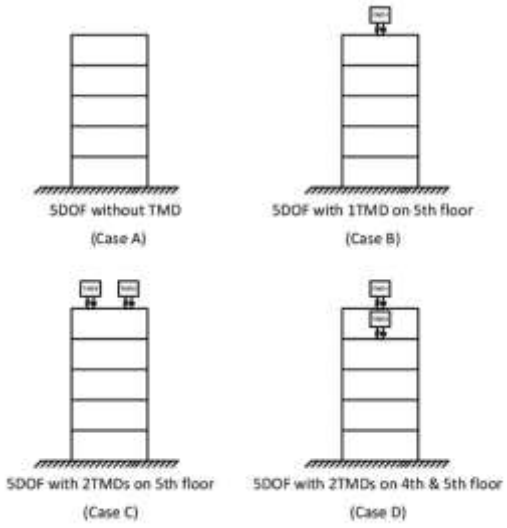

Figure 5. Models of cases analyzed in the present study

The structures were assessed for far-field ground movement datasets, under four earthquake movements recorded in FEMA P-695 (Quantification of Building Seismic Performance Factors) [43]. Table 2 illustrates the seismic details included in this example, such as the closest distance to the fault, duration, magnitude, and peak ground acceleration (PGA). These databases of the earthquake were collected from the Pacific Earthquake Engineering Research Center (PEER) website [44], and the PGAs were scaled to 1g.

Table 1: Earthquake records were used in the analyses and optimization.

ID	Name	Station	Component	Mag	PGA (g)	R (km)
EQ1	Northridge	Beverly Hills	MUL009	6.7	0.44	17.2
EQ2	Hector Mine	Hector	HEC000	7.1	0.27	11.7
EQ3	Kobe, Japan	Nishi-Akashi	NIS000	6.9	0.48	7.1
EQ4	Kobe, Japan	Shin-Osaka	SHI000	6.9	0.22	19.2
EQ5	Friuli, Italy	Tolm ezzo	TMZ000	6.5	0.36	15.8
EQ6	Superstition Hills	Roe Road	POE270	6.5	0.45	11.2

The range of design parameters, including mass and stiffness, for the TMD and MTMDs are as follows: the maximum total mass of the dampers is 172.8 tons, the maximum total stiffness of the dampers is 3.404×10^{8} N/m, and the damping ratio of the dampers is 0.02. The results of analyzing the effectiveness of TMD and MTMD are presented in Table 3.

Table 2: Maximum structural responses and optimum results

ID	Max X_5(m)	M_{d1} (tons)	M_{d2} (tons)	K_{d1} (kN/m)	K_{d2} (kN/m)	% Of red.
			Controlled with 1 TMD (Case B)			
EQ1	0.226	1.35E+02		1.25E+03		11.9
EQ2	0.165	9.01E+00		3.40E+05		2.3
EQ3	0.135	1.11E+02		8.66E+03		34.4
EQ4	0.233	2.54E+01		2.66E+03		8.3
EQ5	0.103	1.64E+02		9.44E+03		37.2
EQ6	0.143	1.54E+02		1.95E+05		31.2
Average	**0.168**	**9.97E+01**		**9.28E+04**		**20.9**
			Controlled with 2 TMDs (Case C)			
EQ1	0.223	1.55E+02	1.06E+01	1.16E+05	2.84E+03	13.0
EQ2	0.126	1.74E-01	1.73E+02	1.98E+05	1.50E+03	25.2
EQ3	0.124	4.10E+01	7.18E+01	3.10E+05	4.88E+03	39.8
EQ4	0.227	1.73E-01	1.25E+01	2.82E+05	6.09E+02	10.7
EQ5	0.104	9.24E+00	1.63E+02	2.99E+05	9.71E+03	45.6
EQ6	0.143	1.39E+02	1.75E+01	2.16E+05	3.82E+04	31.2
Average	**0.158**	**5.74E+01**	**7.47E+01**	**2.37E+05**	**9.62E+03**	**27.6**
			Controlled with 2 TMDs (Case D)			

EQ1	0.206	1.63E+02	4.15E+00	2.42E+03	2.34E+04	19.7
EQ2	0.119	5.00E+01	3.85E+01	1.09E+03	1.09E+03	29.2
EQ3	0.127	1.06E+02	6.32E+01	1.74E+05	1.62E+04	38.2
EQ4	0.222	1.73E+01	1.56E+02	6.96E+02	1.55E+02	12.9
EQ5	0.103	1.72E+02	3.16E-01	1.00E+04	1.15E+04	46.1
EQ6	0.109	1.40E+02	2.09E-01	2.35E+05	2.04E+04	47.4
Average	**0.148**	**1.08E+02**	**4.37E+01**	**7.05E+04**	**1.21E+04**	**32.3**

As shown in Table 3, the minimum impact of TMD on decreasing the building's maximum possible movement was approximately 2.3 percent, while the maximum impact was approximately 47.4 percent. Throughout all near-field earthquakes, the mean impact of the optimized TMDs using the MBF method in Cases (B), (C), and (D) was around 20.9%, 27.6%, and 32.3%, respectively. Based on the maximum displacement of structures presented in Fig. 8, the efficiency of the optimal TMDs on the peak movement of buildings under near-field earthquakes can be seen.

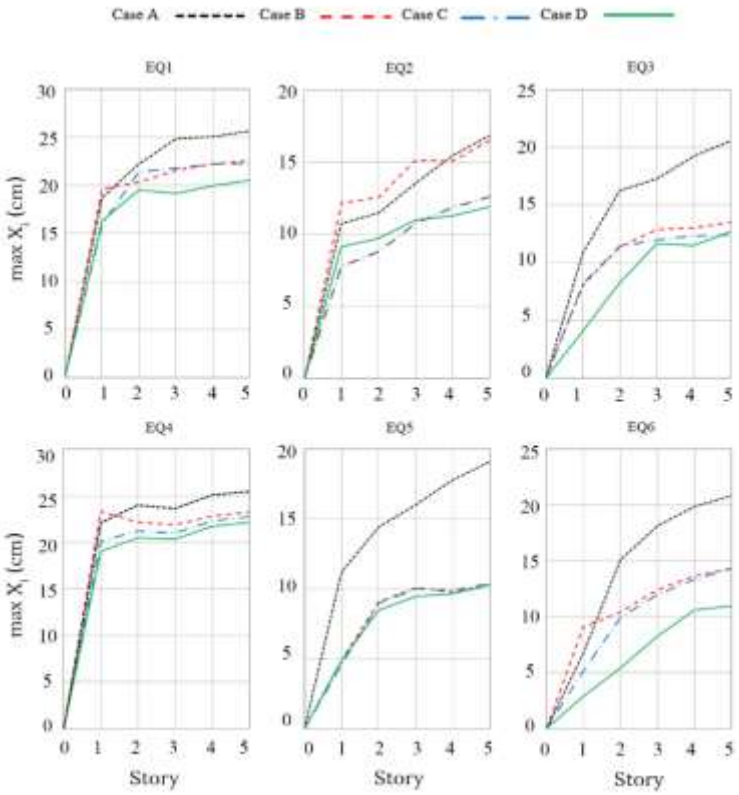

Figure 6. Peak displacement of buildings

7. CONCLUSION

Most of the previous studies have focused on designing multiple optimally tuned mass dampers and have compared the effectiveness of MTMD with TMDs located in linear structures. Hence, in this study, a method has been developed to investigate and compare the effectiveness of TMDs and MTMDs for the mitigation of the responses of nonlinear structures. In doing so, the effectiveness of TMDs and MTMDs on the responses of five-story nonlinear structures equipped with optimal MTMDs and TMDs has been analyzed. According to the results, MTMDs had a great efficiency in decreasing the maximum displacement of nonlinear structure compared to TMDs. Furthermore, MTMDs yield a better effect when placed in different stories compared to the case where both are placed on the top story of the structures.

Declaration of interests

The authors declare that they have no known competing financial interests or personal relationships that could have appeared to influence the work reported in this paper.

Acknowledgments: This research did not receive any specific grant from funding agencies in the public, commercial, or not-for-profit sectors.

REFERENCES

1. Cao Z, Hua X, Wen Q, Chen Z, Niu H. A state space technique for modal identification of coupled structure–tuned mass damper systems from vibration measurement, *Adv Struct Eng* 2019; **22**(9): 2048-60.
2. Chen J, Han Z, Xu R. Effects of human-induced load models on tuned mass damper in reducing floor vibration, *Adv StructEng* 2019; **22**(11): 2449-63.
3. Elias S, Matsagar V. Research developments in vibration control of structures using passive tuned mass dampers, *Annual Rev Control* 2017; **44**: 129-56.
4. Rahman M, Hassan M, Chang S, Kim D. Adaptive multiple tuned mass dampers based on modal parameters for earthquake response reduction in multi-story buildings, *Adv Struct Eng* 2016; **20**(9): 1375-89.
5. Frahm H. Inventor. Device for damping vibrations of bodies, United States patent US 989, 958, 1911.
6. Ormondroyd J, Den Hartog JP. The theory of the dynamic vibration absorber, *ASME J Appl Mech* 1928; **50**(7): 9–22.
7. Sacks MP, Swallow JC. Tuned mass dampers for towers and buildings, *Struct Eng Natural Hazards Mitigat* 1993; 640-5, ASCE.
8. Elias S, Matsagar V. Wind response control of tall buildings with a tuned mass damper, *J Build Eng* 2018; **15**: 51-60.
9. Abd-Elhamed A, Mahmoud S. Simulation analysis of TMD controlled building subjected to far- and near-fault records considering soil-structure interaction, *J Build Eng* 2019; **26**: 100930.
10. Gwalani P, Jaiswal O. Seismic Response Control Using Elastoplastic Tuned Mass Damper.

11. Mohebbi M, Rasouli H, Moradpour S. Assessment of the design criteria effect on performance of multiple tuned mass dampers, *Adv Struct Eng* 2015; **18**(8): 1141-58.
12. Xu K, Igusa T. Dynamic characteristics of multiple substructures with closely spaced frequencies, *Earthq Eng Struct Dyn* 1992; **21**(12): 1059-70.
13. Li C. Optimum multiple tuned mass dampers for structures under the ground acceleration based on DDMF and ADMF, *Earthq Eng Struct Dyn* 2002; **31**(4): 897-919.
14. Zuo L. Effective and robust vibration control using series multiple tuned-mass dampers, *J Vib Acoustic* 2009; **131**(3).
15. Steinbuch R. Bionic optimization of the earthquake resistance of high buildings by tuned mass dampers, *J Bionic Eng* 2011; **8**(3): 335-44.
16. Mohebbi M, Shakeri K, Ghanbarpour Y, Majzoub H. Designing optimal multiple tuned mass dampers using genetic algorithms (GAs) for mitigating the seismic response of structures, *J Vib Control* 2012; **19**(4): 605-25.
17. Frans R, Arfiadi Y. Designing optimum locations and properties of MTMD systems, *Proced Eng* 2015; **125**: 892-8.
18. Sakr T. Vibration control of buildings by using partial floor loads as multiple tuned mass dampers, *HBRC J* 2017; **13**(2): 133-44.
19. Rahman M, Hassan M, Chang S, Kim D. Adaptive multiple tuned mass dampers based on modal parameters for earthquake response reduction in multi-story buildings, *Adv Struct Eng* 2016; **20**(9): 1375-89.
20. Suresh L, Mini K. effect of multiple tuned mass dampers for vibration control in high-rise buildings, *Pract Period Struct Des Construct* 2019; **24**(4): 04019031.
21. Lewandowski R, Grzymisławska J. Dynamic analysis of structures with multiple tuned mass dampers, *J Civil Eng Manag* 2009; **15**(1): 77-86.
22. Chopra AK. Theory and Applications to earthquake engineering, *Dyn Struct* 1995.
23. Jahani E, Chizari M. Tackling global optimization problems with a novel algorithm – Mouth Brooding Fish algorithm, *Appl Soft Comput* 2018; **62**: 987-1002.
24. Tan Y, Yao Y. Optimization of hanger arrangement in pedestrian tied arch bridge with sparse hanger system, *Adv Struct Eng* 2019; **22**(12): 2594-2604.
25. Dadkhah H, Mohebbi M. Performance assessment of an earthquake-based optimally designed fluid viscous damper under blast loading, *Adv Struct Eng* 2019; **22**(14): 3011-25.
26. Xu Y, Guo T, Yan P. Design optimization of triple friction pendulums for base-isolated high-rise buildings, *Advances in Structural Engineering.* 2019; **22**(13): 2727-40.
27. Huang M, Lei Y, Cheng S. Damage identification of bridge structure considering temperature variations based on particle swarm optimization - cuckoo search algorithm, *Adv Struct Eng* 2019; **22**(15): 3262-76.
28. Yang D, Frangopol D, Teng J. Probabilistic life-cycle optimization of durability-enhancing maintenance actions: Application to FRP strengthening planning, *Eng Struct* 2019; **188**: 340-9.
29. Awad H, Salim K, Gül M. Multi-objective design of grid-tied solar photovoltaics for commercial flat rooftops using particle swarm optimization algorithm, *J Build Eng* 2020; **28**: 101080.
30. Uz M, Sharafi P, Askarian M, Fu W, Zhang C. Automated layout design of multi-span reinforced concrete beams using charged system search algorithm, *Eng Computat* 2018; **35**(3): 1402-13.
31. Kaveh A, Khodadadi N, Azar BF, Talatahari S. Optimal design of large-scale frames with an advanced charged system search algorithm using box-shaped sections, *Eng Comput* 2020: 1-21.

32. Xu H, Liu J, Lu Z. Structural damage identification based on cuckoo search algorithm, *Adv Struct Eng* 2016; **19**(5): 849-59.
33. Tran-Ngoc H, Khatir S, De Roeck G, Bui-Tien T, Abdel Wahab M. An efficient artificial neural network for damage detection in bridges and beam-like structures by improving training parameters using cuckoo search algorithm, *Eng Struct* 2019; **199**: 109637.
34. Zhang H, Zhang L. Tuned mass damper system of high-rise intake towers optimized by improved harmony search algorithm, *Eng Struct* 2017; **138**: 270-82.
35. Molina-Moreno F, García-Segura T, Martí J, Yepes V. Optimization of buttressed earth-retaining walls using hybrid harmony search algorithms, *Eng Struct* 2017; **134**: 205-16.
36. Hadi M, Arfiadi Y. Optimum Design of Absorber for MDOF Structures, *Adv Struct Eng*; **124**(11): 1272-80.
37. Kaveh A, Mohammadi S, Hosseini OK, Keyhani A, Kalatjari VR. Optimum parameters of tuned mass dampers for seismic applications using charged system search, *Iranian J Sci Technol, Transact Civil Eng* 2015; **39**(C1): 21.
38. Etedali S, Rakhshani H. Optimum design of tuned mass dampers using multi-objective cuckoo search for buildings under seismic excitations, *Alexandria Eng J* 2018; **57**(4): 3205-18.
39. Yazdi H, Saberi H, Saberi H, Hatami F. Designing optimal tuned mass dampers using improved harmony search algorithm, *Adv Struct Eng* 2016; **19**(10): 1620-36.
40. Yucel M, Bekdaş G, Nigdeli S, Sevgen S. Estimation of optimum tuned mass damper parameters via machine learning, *J Build Eng* 2019; **26**: 100847.
41. Jangid RS. *Introduction to Earthquake Engineering*, 2014.
42. Mohebbi M, Joghataie A. Designing optimal tuned mass dampers for nonlinear frames by distributed genetic algorithms, *Struct Des Tall Special Build* 2011; **21**(1): 57-76.
43. Quantification of building seismic performance factors, Washington, D.C, U.S. Department of Homeland Security, FEMA, 2009.
44. PEER Ground Motion Database - PEER Center [Internet]. Ngawest2.berkeley.edu. 2020 [cited 1 October 2020]. Available from: https://ngawest2.berkeley.edu/.